Journal of Coordination Chemistry

ISSN: 0095-8972 (Print) 1029-0389 (Online) Journal homepage: http://www.tandfonline.com/loi/gcoo20

Asymmetric bis-($\mu_{1,1}$-azido) bridged dinuclear copper(II) complex with N_2O donor Schiff base: synthesis, structure and magnetic study

Mithun Das, Bikash Kumar Shaw, Biswa Nath Ghosh, Kari Rissanen, Shyamal Kumar Saha & Shouvik Chattopadhyay

To cite this article: Mithun Das, Bikash Kumar Shaw, Biswa Nath Ghosh, Kari Rissanen, Shyamal Kumar Saha & Shouvik Chattopadhyay (2015) Asymmetric bis-($\mu_{1,1}$-azido) bridged dinuclear copper(II) complex with N_2O donor Schiff base: synthesis, structure and magnetic study, Journal of Coordination Chemistry, 68:8, 1361-1373, DOI: 10.1080/00958972.2015.1014350

To link to this article: http://dx.doi.org/10.1080/00958972.2015.1014350

Accepted author version posted online: 05 Feb 2015.
Published online: 20 Mar 2015.

Journal of Coordination Chemistry, 2015
Vol. 68, No. 8, 1361–1373, http://dx.doi.org/10.1080/00958972.2015.1014350

Asymmetric bis-($\mu_{1,1}$-azido) bridged dinuclear copper(II) complex with N_2O donor Schiff base: synthesis, structure and magnetic study

MITHUN DAS†, BIKASH KUMAR SHAW‡, BISWA NATH GHOSH§, KARI RISSANEN§, SHYAMAL KUMAR SAHA‡ and SHOUVIK CHATTOPADHYAY*†

†Department of Chemistry, Inorganic Section, Jadavpur University, Kolkata, India
‡Department of Materials Science, Indian Association for the Cultivation of Science, Kolkata, India
§Department of Chemistry, Nanoscience Center, University of Jyväskylä, Jyväskylä, Finland

(*Received 28 October 2014; accepted 15 January 2015*)

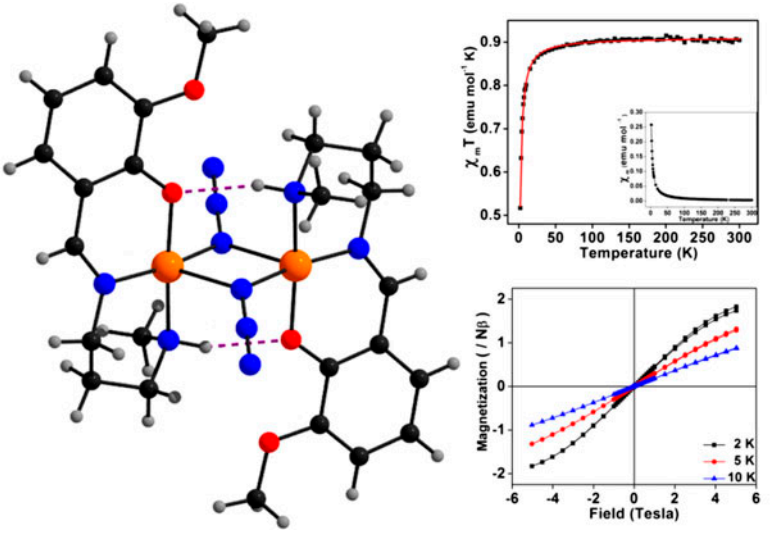

A double end-on azide-bridged centrosymmetric dinuclear copper(II) complex, $[Cu_2(L)_2(N_3)_2]$, has been synthesized and characterized. X-ray crystal structure analysis has confirmed the structure; variable temperature (2–300 K) magnetic susceptibility measurement indicates antiferromagnetic exchange interactions with $2J = -0.45$ cm^{-1}.

A copper(II) complex, *$[Cu_2(L)_2(N_3)_2]$* [where HL = *2-((3-(methylamino)propylimino)methyl)-6-methoxyphenol*] has been synthesized and characterized by elemental analysis, IR, UV–vis and fluorescence spectroscopy, and single-crystal X-ray diffraction studies. The complex crystallizes in the trigonal space group $R\bar{3}$. The deprotonated tridentate Schiff base occupies three coordination sites of

*Corresponding author. Email: shouvik.chem@gmail.com

copper(II). The fourth coordination site is occupied by an azide. A symmetry-related azide from a different molecule coordinates with the fifth site of copper(II), thereby forming a double end-on azide-bridged centrosymmetric dimer. Variable temperature solid–state magnetic studies between 2 and 300 K were carried out and the data indicate predominant antiferromagnetic exchange interactions with $2J = -0.45$ cm^{-1}. The magnetic field-dependent magnetization study (M − H) reveals existence of antiferromagnetic ordering at a lower temperature (2 K) with a very small coercive field (~20 Oe) suggesting soft magnet behavior of the complex.

Keywords: Schiff base; Copper(II); Dinuclear; Antiferromagnetic; Field-dependent magnetization study

1. Introduction

The synthesis and characterization of di- and polynuclear copper(II) complexes have attracted interest due to their relevance in understanding the magneto-structural correlations arising from exchange coupling among copper(II) centers. Azide is a popular bridging ligand in forming di- and polynuclear complexes with diverse architectures and interesting magnetic properties [1–5]. Active Jahn–Teller effects on the copper(II) center makes the structures even more versatile [4–6]. Magnetic exchange via the azide bridge can be ferro- or antiferromagnetic, depending upon the bridging mode and bonding parameters [6–8]. Thus, magnetic interactions mediated by an azide bridge are genearally antiferromagnetic for the end-to-end bridging mode ($\mu_{1,1}$-N_3), and ferromagnetic interaction for end-on bridging mode ($\mu_{1,3}$-N_3), provided the bridging angle is small [9–11]. However, ferromagnetic coupling decreases with increase in bridging Cu–N–Cu angle and end-on azide bridge propagates antiferromagnetic coupling with relatively large (~104° or more) bridging Cu–N–Cu angle [12].

N_2O donor tridentate Schiff bases are popularly used as blocking ligands in forming such pseudohalide-bridged di- and polynuclear copper(II) complexes [13–15]. The ease of synthesis and stability under a variety of conditions contributes to popularity of the N_2O donor tridentate Schiff bases. The ability of the phenoxo oxygen to form bridges may be another reason to choose them in forming di- and polynuclear complexes with interesting structures. The phenoxo oxygen may also participate in hydrogen bonding, which in turn, may influence the magnetic coupling among the paramagnetic centers [16]. We have used a tridentate Schiff base, *HL,* (*2-((3-(methylamino)propylimino)methyl)-6-methoxyphenol*), as blocking ligand to form bis-($\mu_{1,1}$-azido)-bridged dinuclear copper(II) complex having very low bridging angle (91.24°). Such a low bridging angle usually favors ferromagnetic coupling among the copper(II) centers [17]. This argument is not at all true for $\mu_{1,1}$-azide-bridged dinuclear copper(II) complexes with tridentate chelating blocking ligands because in such complexes, $\mu_{1,1}$-azide bridges connect an axial position of one copper(II) with a basal one of another and therefore, the overlap of the magnetic orbitals is almost negligible [18]. We have used a tridentate Schiff base blocking ligand in preparing a double $\mu_{1,1}$-azide-bridged dinuclear copper(II) complex. The structure of the complex has been confirmed by single-crystal X-ray diffraction study. Variable temperature magnetic susceptibility measurement indicates the presence of weak antiferromagnetic interaction among the copper(II) centers in the dinuclear entity. The present complex does not have significant $\pi\cdots\pi$ interactions, and forms a 3-D architecture only via C–H$\cdots\pi$ interactions. The magnetic field dependent magnetization study indicates antiferromagnetic ordering at a lower temperature (2 K) with very small coercive field (~20 Oe) suggesting, soft magnet behavior of the complex. Although,

field-induced long-range ordering via $\pi\cdots\pi$ interactions is observed in many systems [19, 20], such ordering via C–H$\cdots\pi$ interaction is not very common. Herein, we report the synthesis, spectroscopic characterization, X-ray crystal structure analysis, and magnetic study of an asymmetric bis-($\mu_{1,1}$-azido) bridged dinuclear copper(II) complex with a N_2O donor Schiff base.

2. Experimental

2.1. *Materials*

All chemicals were of reagent grade and purchased from Sigma-Aldrich. They were used without purification.

Caution!!! Since azide compounds of metal ions are potentially explosive, only small amounts of the materials should be handled with care.

2.2. *Preparation of complex [$Cu_2L_2(N_3)_2$]*

A methanol solution (20 mL) of 3-methoxysalicylaldehyde (153 mg, 1 mmol) and N-methyl-1, 3-diaminopropane (0.1 mL, 1 mmol) was refluxed for ca. 30 min to produce *HL* following the literature method [21]. Then methanol solution of *HL* was added to the suspension of copper(II) acetate monohydrate (1 mmol, 370 mg) in methanol (10 mL) and stirred for 1 h. A methanol–water (2 : 1) solution (10 mL) of sodium azide (1 mmol, 65 mg) was added and refluxed for an additional 2 h. The resulting dark green solution was set aside at room temperature. Single-crystals, suitable for X-ray diffraction, were obtained from the reaction mixture on slow evaporation in open atmosphere. (Yield: 240 mg, 73%). Anal. Calcd for $C_{24}H_{34}Cu_2N_{10}O_4$ (653.69): C, 44.10; H, 5.24; N, 21.43%. Found: C, 44.3; H, 5.4; N, 21.2%. IR (cm^{-1}): 3378 (NH); 2050 (N_3); 1614 (C=N). UV–vis, λ_{max} (nm) [ε_{max} (LM^{-1} cm^{-1})] (CH_3CN): 379 (3020), 671 (294).

2.3. *Physical measurements*

Elemental analysis was performed on a PerkinElmer 240C elemental analyzer. IR spectra in KBr (4500–500 cm^{-1}) were recorded using a PerkinElmer Spectrum Two FT-IR spectrophotometer. Electronic spectra in acetonitrile (800–300 nm) were recorded in a PerkinElmer LAMBDA 35 UV/Vis spectrophotometer. Fluorescence spectra were obtained on a SHIMADZU RF-5301PC Spectrofluorophotometer at room temperature. SQUID magnetometer (Quantum Design MPMS) was used to investigate the magnetic properties [magnetic susceptibility (field cooled magnetization) and magnetic field dependent magnetization measurements].

2.4. *X-ray crystallography*

The structural analysis of the complex was performed on an Agilent SuperNova diffractometer with Atlas detector using mirror monochromated Mo-*K*α (λ = 0.71073 Å) radiation at 173 K. *CrysAlisPro* program was used for data collection and processing [22]. The intensities were corrected for absorption using the *analytical face index absorption correction*

method [23]. The structure was solved by charge flipping method with *SUPERFLIP* [24] and refined by full-matrix least-squares methods using the *WinGX-software* [25], which utilizes the *SHELXL-97* module [26]. All non-hydrogen atoms were refined with anisotropic thermal parameters. Hydrogens were introduced in proper positions with isotopic thermal parameters using the 'riding model.' ORTEP figures were plotted using *Ortep-3 for Windows* [27], and structures were analyzed with *Mercury* v 2.3 [28]. Significant crystallographic data are summarized in table 1.

2.5. *Hirshfeld surface analysis*

Hirshfeld surfaces [29–31] and the associated 2-D fingerprint [32–34] plots were calculated using Crystal Explorer [35], which accepted a structure input file in CIF format. Bond lengths for hydrogens were set to standard values. For each point on the Hirshfeld isosurface, two distances d_e, the distance from the point to the nearest nucleus external to the surface, and d_i, the distance to the nearest nucleus internal to the surface were defined. The normalized contact distance (d_{norm}) based on d_e and d_i is given by

$$d_{norm} = \frac{(d_i - r_i^{vdw})}{r_i^{vwd}} + \frac{(d_e - r_e^{vdw})}{r_e^{vwd}}$$

where r_i^{vdW} and r_e^{vdW} are the van der Waals radii of the atoms. The value of d_{norm} was negative or positive depending on intermolecular contacts being shorter or longer than the van der Waals separations. The parameter d_{norm} displayed a surface with a red–white–blue color scheme, where bright red spots highlighted shorter contacts, white areas represented contacts around the van der Waals separation, and blue regions were devoid of close contacts. For a given crystal structure and set of spherical atomic electron densities, the Hirshfeld surface was unique [36] and it was this property that suggested the possibility of gaining additional insights into the intermolecular interaction of molecular crystals.

Table 1. Crystal data and refinement details of the complex.

Formula	$C_{24}H_{34}Cu_2N_{10}O_4$
Formula weight	653.69
Crystal size (mm)	0.21 × 0.29 × 0.34
Temperature (K)	173
Crystal system	Trigonal
Space group	$R\bar{3}$
a (Å)	27.9734(7)
b (Å)	27.9734(7)
c (Å)	9.3941(2)
Z	9
d_{calc} (g cm^{-3})	1.535
μ(mm^{-1})	1.553
F(0 0 0)	3042
Total reflections	4253
Unique reflections	2616
Observed data [$I > 2\sigma(I)$]	2400
R(int)	0.014
R_1, wR_2 (all data)	0.0275, 0.0614
R_1, wR_2 [$I > 2\sigma(I)$]	0.0242, 0.0595
Largest difference in peak and hole (e Å^{-3})	0.26, −0.30

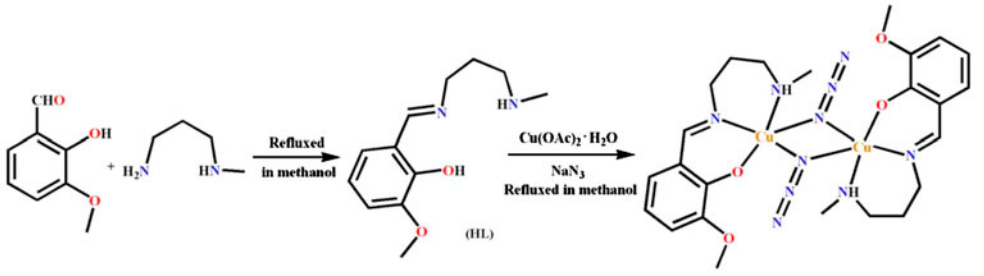

Scheme 1. Synthesis of the complex.

Table 2. Structural (distances in Å and angles in °) and magnetic parameters (J in cm^{-1}) of double $\mu_{1,1}$-N_3 bridged copper(II) complexes.

Complex	g	$2J$	Cu···Cu	Cu–N	Cu–N–Cu	Reference
$[Cu_2(L)_2(N_3)_2]$ (1)	2.10	–0.45	3.1122(3)	2.035(2), 2.311(2)	91.24(6)	This work
$[Cu_2(L^1)_2(N_3)_2]\cdot DMF$	2.12	+19.2	3.1785(8), 3.1822(7)	1.984(4), 2.646(4), 1.995 (3), 2.577(4)	85.4(1), 87.2 (1)	[42]
$[Cu_2(L^2)_2(N_3)_2]$	2.13	−24.7	3.4259(3)	2.009(1), 2.374(2)	102.50(7)	[42]
$[Cu_2(L^4)_2(N_3)_2]$	2.12	−11.4	3.3703(5)	2.404(2), 1.968(2)	100.40(8)	[42]
$[Cu_2(L^8)_2(N_3)_2]$	2.11	–3.6	3.193	2.039(7), 2.440(7)	90.50	[43]
$[Cu_2(L^9)_2(N_3)_2]$	2.12	–6.2	3.161	2.020(4), 2.546(5)	86.82	[43]
$[Cu_2(L^{10})_2(N_3)_2]$	2.11	+5.8	3.318	2.060(8), 2.475(9)	93.60	[43]
$[Cu_2(L^{11})_2(N_3)_2]$	2.10	–5.18	3.168(1)	2.059(2), 2.338(2)	91.95(9)	[44]
$[Cu_2(L^{11})_2(N_3)_2]\cdot H_2O$	2.07	–0.20	3.3232(5)	2.045, 2.354(2), 2.060(2), 2.339	97.87(8), 97.93(9)	[44]
$[Cu_2(dipn)_2(N_3)_2]$	2.05	–4.20	3.370(1)	2.023(3), 2.617(4)	92.2(1)	[45]
$[Cu_2(L^{12})_2(N_3)_2]$	2.10	–17.0	3.181(1)	1.998(3), 2.505(3)	89.1	[46]
$[Cu_2(L^5)_2(N_3)_2]$	–	–	3.702(2)	1.961(3), 2.800(3)	100.6(1)	[47]
$[Cu_2(L^6)_2(N_3)_2]$	–	–	3.143(2)	2.464(3), 1.977(3)	89.4(1)	[47]
$[Cu_2(L^7)_2(N_3)_2]$	–	–	3.352(2)	2.348(2), 2.007(2)	100.35(7)	[48]
$[Cu_2(L^{13})_2(N_3)_2]\cdot MeOH$	–	–	3.306(2)	2.342(5), 2.356(5), 2.018 (4), 2.048(5)	94.4(2), 80.4 (2)	[49]
$[Cu_2(IEP)_2(N_3)_2]$	–	–	3.230(2)	2.003(4), 2.417(4)	93.4(2)	[50]
$[Cu_2(EMP)_2(N_3)_2]$	–	–	3.150(2)	1.989(3), 2.510(4)	88.1(1)	[50]
$[Cu_2(L^{14})_2(N_3)_2]$	–	–	3.1925(7)	2.059(3), 2.451(3)	89.7(1)	[51]
$[Cu_2(L^{15})_2(N_3)_2]$	–	–	3.566	2.005(6), 2.508(6)	103.8(3)	[52]
$[Cu_2(L^{16})_2(N_3)_2]$	–	–	3.368(1)	1.982(2), 2.557(2)	94.97(9)	[53]

Notes: HL^1 = 1-((2-aminopropylimino)methyl)naphthalen-2-ol.
HL^2 = 1-(1-(3-(dimethylamino)propylimino)ethyl)naphthalen-2-ol.
HL^4 = 1-(1-(2-(diethylamino)ethylimino)ethyl)naphthalen-2-ol.
HL^8 = N-(3-aminopropyl)salicylaldimine.
HL^9 = 7-amino-4-methyl-5-azahept-3-en-2-one.
HL^{10} = 8-amino-4-methyl-5-azaoct-3-en-2-one.
HL^{11} = 2-((3-methylaminopropylimino)methyl)phenol.
Hdipn = 4-((3-aminopentylimino)-methyl)-benzene-1,3-diol.
HL^{12} = 2-((2-aminoethylimino)methyl)phenol.
HL^5 = 4-bromo-2-((2-diethylaminoethylimino)methyl)phenol.
HL^6 = 1-((2-ethylaminoethylimino)methyl)-naphthalene-2-ol.
HL^7 = 1-((3-dimethylaminopropylimino)methyl)naphthalen-2-ol.
HL^{13} = 2-((3-methylaminopropylimino)methyl)phenol.
HIEP = 2-(1-(2-isopropylaminoethylimino)ethyl)phenol.
HEMP = 2-ethoxy-6-((2-methylaminoethylimino)methyl)phenol.
HL^{14} = 2-(1-(3-aminopentylimino)ethyl)phenol.
HL^{15} = 6-diethylamino-3-methyl-1-phenyl-4-azahex-3-en-1-one.
HL^{16} = 1-((pyridin-2-ylmethylimino)methyl)naphthalen-2-ol.

3. Results and discussion

3.1. *Synthesis*

The Schiff base ligand, *HL* (*2-((3-(methylamino)propylimino)methyl)-6-methoxyphenol*) was prepared by 1 : 1 condensation of 3-methoxysalicylaldehyde with N-methyl-1,3-diaminopropane in methanol following the literature method [21]. The methanol solution was then reacted with copper(II) acetate monohydrate and sodium azide to produce a double $\mu_{1,1}$-N_3-bridged dinuclear copper(II) complex (scheme 1). Several groups have reported many such di- and polynuclear copper(II) complexes bridged by azide or similar ligands [37–53]. Table 2 gathers all such double $\mu_{1,1}$-N_3-bridged dinuclear copper(II) complexes with tridentate N_2O donor Schiff bases.

3.2. *Structure description*

The complex crystallizes in trigonal space group $R\bar{3}$ and features a double end-on azide-bridged centrosymmetric copper(II) dimer as shown in figure 1. Copper(II) is five-coordinate. The geometry of five-coordinate metal centers may be measured by the Addison parameter (τ), which is 0.0265 in this case [$\tau = (\alpha - \beta)/60$, where, α and β are the two largest ligand–metal–ligand angles of the coordination sphere], suggesting square pyramidal geometry ($\tau = 0$ for perfect square pyramid and $\tau = 1$ for perfect trigonal bipyramid) [54]. Copper(II) is coordinated by two nitrogens, N(1) and N(2), and one oxygen, O(1), of the deprotonated ligand $(L)^-$, and one azide nitrogen, N(3), in the equatorial plane. The apical fifth coordination site of the square pyramid is occupied by N(3)*, of the symmetry related azide ($^* = 1 - x, 1 - y, 2 - z$). Selected bond lengths and angles are listed in table 3.

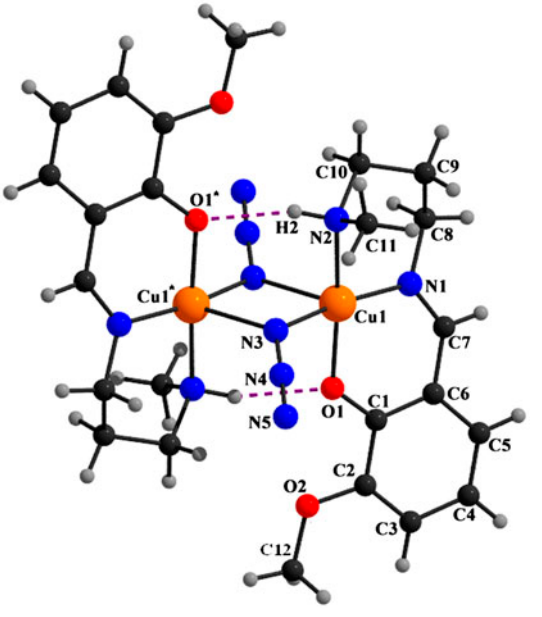

Figure 1. A perspective view of the complex with atom numbering scheme (except hydrogens). Hydrogens are shown as spheres of arbitrary radius.

Table 3. Selected bond lengths (Å) and angles (°) around copper(II).

Bond lengths		Bond angles			
Cu(1)–O(1)	1.920(2)	O(1)–Cu(1)–N(1)	92.15(7)	N(1)–Cu(1)–N(3)	169.40(6)
Cu(1)–N(1)	1.979(2)	O(1)–Cu(1)–N(2)	170.99(7)	N(1)–Cu(1)–N(3)[a]	101.73(7)
Cu(1)–N(2)	2.023(2)	O(1)–Cu(1)–N(3)	86.50(7)	N(2)–Cu(1)–N(3)	84.80(7)
Cu(1)–N(3)	2.035(2)	O(1)–Cu(1)–N(3)[a]	88.74(6)	N(2)–Cu(1)–N(3)[a]	93.37(7)
Cu(1)–N(3)[a]	2.311(2)	N(1)–Cu(1)–N(2)	95.98(7)	N(3)–Cu(1)–N(3)[a]	88.76(6)

Symmetry transformation: [a] = 1 − *x*, 1 − *y*, and 2 − *z*.

The interdimer bridging angle {Cu(1)–N(1)–Cu(1)*} and copper(II)···copper(II) distance {Cu(1)···Cu(1)*} are 91.24(6)° and 3.1122(3) Å, respectively. The deviations of N(1), N(2), N(3), and O(1), from the mean square basal plane are 0.062(2), −0.063(2), 0.069(2), and −0.068(1), respectively. As usual for a square pyramid structure, the copper(II) is slightly pulled out of the mean-square plane toward the apical donor N(3)* by 0.1189(2) Å. The six-membered ring, Cu(1)–N(1)–C(8)–C(9)–C(10)–N(2), has an intermediate conformation between envelope and half-chair with puckering parameters q(2) = 0.542(2) Å, $\theta(2)$ = 26.2 (2)°, and $\phi(2)$ = 191.6 (5)° [55].

H(2) is available in the ligand for hydrogen bonding with a symmetry-related (* = 1 − *x*, 1 − *y*, 2 − *z*) phenolic oxygen, O(1)* (figure 1), where ∠N(2)–H(2)···O(1)* angle is 154° and N(2)–H(2), H(2)···O(1)*, N(2)···O(1)* distances are 0.93, 2.12, and 2.987(2) Å, espectively.

H(8B) attached with C(8) forms C–H···π interaction with the phenyl ring **R**^{4} [C(1)–C(2)–C(3)–C(4)–C(5)–C(6)]. One aromatic hydrogen, H(3) attached with C(3) forms another C–H···π interaction with the same phenyl ring **R**^{4} (figure 2). Considering the centrosymmetric dimer each of these interactions is duplicated and the combination of those interactions creates a 3-D supramolecular structure as shown in figure 3. Geometric features of the C–H···π interactions are given in table 4.

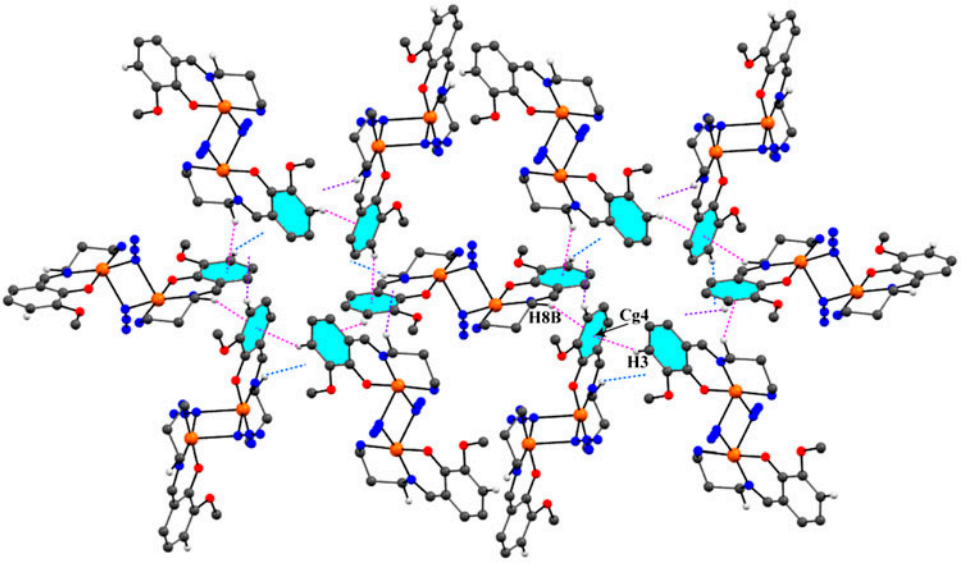

Figure 2. A perspective view of C–H···π interactions in the crystalline architecture of the complex.

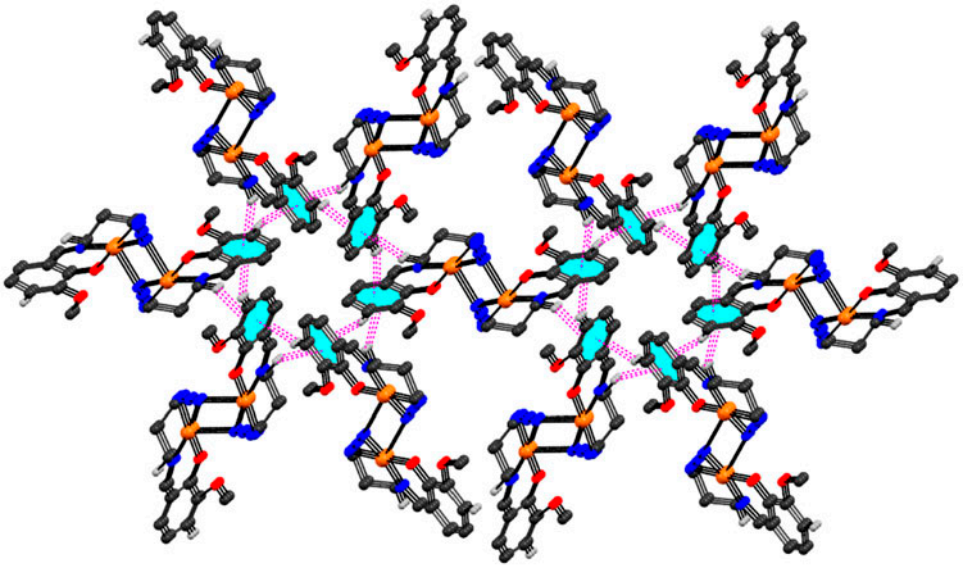

Figure 3. A perspective view of the 3-D supramolecular network within the complex via C–H···π interactions.

3.4. *IR and electronic spectra and photophysical study*

A distinct band due to azomethine (C=N) at 1614 cm^{-1} is in the IR spectrum [56]. Appearance of a strong band at 2050 cm^{-1} indicates the presence of azide [57]. The sharp band due to amino NH appears at 3378 cm^{-1} [58]. The electronic spectrum of the complex shows absorption at 671 nm, which is assigned as d–d transition of square pyramidal copper(II) center [59]. Another high energy band is observed at 379 nm, which is assigned as LMCT, and characteristic of transition metal complexes with Schiff base ligands [60]. The complex exhibits emission at 424 nm in the visible region upon irradiation with UV light (379 nm) in acetonitrile at room temperature. This emission band can be attributed to intra-ligand fluorescent $^1(\pi \rightarrow \pi^*)$ emission of the coordinated ligand [61].

3.5. *Powder XRD*

The experimental PXRD pattern of the bulk product is in agreement with the simulated XRD pattern from single-crystal X-ray diffraction, indicating consistency of the bulk sample (figure 4). The simulated pattern of the complex is calculated from the single crystal structural data (cif files) using CCDC Mercury software.

Table 4. Geometric features (distances in Å and angles in °) of the C–H···π interactions obtained for the complex.

C–H···Cg (ring)	H···Cg (Å)	C–H···Cg (°)	C···Cg (Å)
C(3)–H(3)···Cg(4)	2.679	152.66	3.550
C(8)–H(8B)···Cg(4)	2.662	151.13	3.562

Note: Cg(4) = Center of gravity of the ring $\mathbf{R^4}$ [C(1)–C(2)–C(3)–C(4)–C(5)–C(6)].

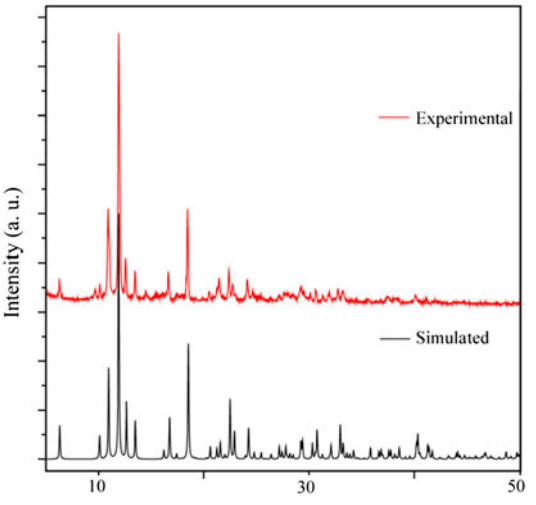

Figure 4. Experimental and simulated powder XRD patterns of complex.

3.6. *Hirshfeld surfaces*

Figure 5 illustrates the Hirshfeld surface of the complex, mapped over d_{norm} (range of −0.1 to 1.5 Å). The surface is shown as transparent, to allow visualization of the molecular moiety around which it is calculated. The dominant interaction between oxygen and hydrogen can be observed in the Hirshfeld surface as red areas in figure 5(A). Other visible spots correspond to the presence of C–H···π interactions. The small area and light color on the surface indicate weaker and longer contact other than hydrogen bonds. Complementary region is visible in the fingerprint plot [figure 5(B)], where one molecule acts as donor ($d_e > d_i$) and the other as an acceptor ($d_e < d_i$). The proportion of O···H/H···O interactions comprises 11.2% of the Hirshfeld surface of the complex [62].

3.7. *Magnetic properties*

Temperature dependent magnetic susceptibility (field-cooled magnetization) of the complex is investigated under the applied magnetic field of 100 Oe from 2 to 300 K as shown in the inset of figure 6. The susceptibility increases upon cooling, and rises suddenly at temperatures below 45 K. Figure 6 displays the variation of $\chi_M T$ as a function of temperature which shows the continuous decrease of $\chi_M T$ from 0.91 to 0.88 $cm^3\ M^{-1}\ K$ till 45 K, and falls rapidly in the lower temperature region to 0.51 $cm^3\ M^{-1}\ K$ at 2 K. This behavior indicates the presence of weak antiferromagnetic exchange interactions between copper(II).

The experimental data for magnetic susceptibility with temperature is fitted in the form of the variation of $\chi_M T$ *versus* T using the theoretical expression of dinuclear systems given by

$$\chi_M = \frac{(2N\beta^2 g^2)}{k(T-\theta)}[3 + \exp(-2J/kT)]^{-1} \quad (1)$$

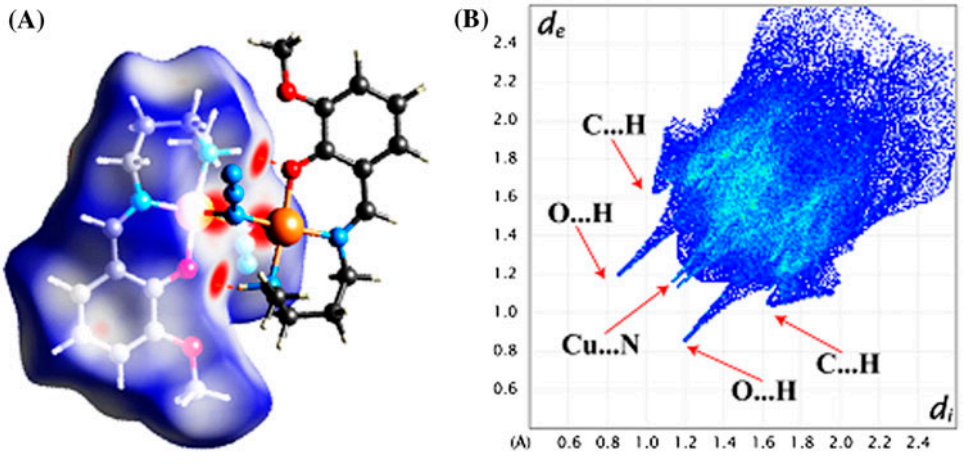

Figure 5. A perspective views of (A) Hirshfeld surfaces mapped over d_{norm} and (B) full fingerprint plots of the complex.

where N, β, and k are constants and have their usual significance [63]. The values of g, θ, and $2J$ (singlet–triplet energy gap) parameters, and the corresponding agreement factors (R^2), $\sum T^2(\chi_{obs} - \chi_{cal})^2 \Big/ \sum T^2(\chi_{obs})^2$ obtained from the least squares fitting procedure, are 2.10, −0.93, −0.45, and 4.8×10^{-5}, respectively.

From the fitted curve, the susceptibility follows weak antiferromagnetic exchange pathway between the intra-dimer copper(II) with negative exchange coupling constant value, $2J = -0.45$ cm^{-1}. The Cu–($\mu_{1,1}$–N_3)–Cu bridge angle of 91.24(6)°, generally shows ferromagnetic interactions between copper(II), but very low negative value of singlet–triplet energy gap ($2J$) obtained from the fitting procedure reveal antiferromagnetic interactions between the copper(II). This contradiction mainly concludes predominant stabilization of singlet ground state over the triplet state at very low temperatures. The magnetic field

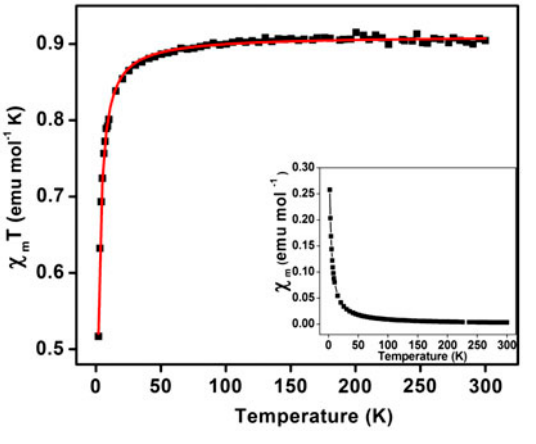

Figure 6. A plot of χ_M (inset) and $\chi_M T$ *vs.* T for the complex. The solid line in red represents the best fit curve (see http://dx.doi.org/10.1080/00958972.2015.1014350 for color version).

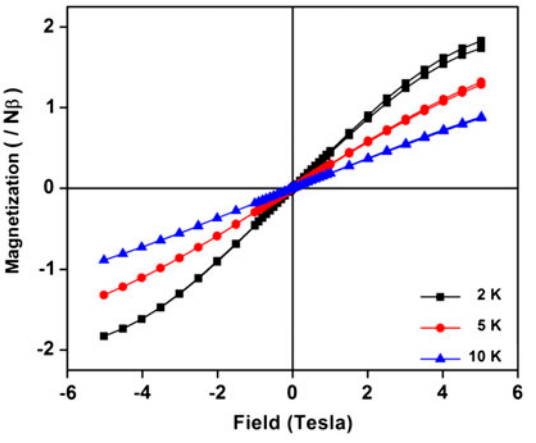

Figure 7. Change in magnetization with magnetic field (up to 5 Tesla) at different temperatures.

dependent magnetization (M − H) was carried out over the temperature range from 2 to 300 K. Figure 7 shows the variation of magnetization ($N\beta$) with field upto 10 K. From figure 7 at 2 K an 's'- shaped magnetization curve is obtained, which becomes unsaturated at a higher field (5 Tesla). This is due to the existence of antiferromagnetic ordering at lower temperatures. The very small coercive field (H_c) around 20 Oe also signifies the behavior of a soft magnet. The magnetization behavior becomes linear paramagnetic type with increase in temperature.

4. Summary

The synthesis and characterization of a double end-on azide bridged dinuclear copper(II) complex with a N_2O donor tridentate Schiff base have been described in the present article. X-ray crystal structure determination confirmed the structure of the complex. Variable temperature magnetic susceptibility measurements showed the presence of antiferromagnetic interaction among the copper(II) centers in the complex. The complex forms a 3-D supramolecular architecture via C–H$\cdots\pi$ interactions. The magnetic field dependent magnetization study (M − H) reveals antiferromagnetic ordering at a lower temperature (2 K) with very small coercive field (~20 Oe), suggesting soft magnet behavior of the complex. As the present complex does not have any significant $\pi\cdots\pi$ interactions, it could be cited as an example of copper(II) complex showing long-range magnetic ordering via C–H$\cdots\pi$ interactions.

Supplementary material

CCDC 1007150 contains the supplementary crystallographic data for complex. The data can be obtained free of charge via http://www.ccdc.cam.ac.uk/conts/retrieving.html or from the Cambridge Crystallographic Data Centre, 12 Union Road, Cambridge CB2 1EZ, UK; fax: (+44) 1223-336-033; or e-mail: deposit@ccdc.cam.ac.uk.

Acknowledgments

SC acknowledges DST, India under FAST Track Scheme (Order No. SR/FT/CS-118/2010, dated 15/02/2012). SKS acknowledges DST, India (project No. SR/NM/NS-1089/2011) for providing facilities of magnetic measurements. BKS acknowledges CSIR, New Delhi, for awarding fellowship.

References

[1] M. Das, S. Chatterjee, S. Chattopadhyay. *Polyhedron*, **68**, 205 (2014).
[2] L. Yang, S. Zhang, X. Liu, Q. Yang, Q. Wei, G. Xie, S. Chen. *CrystEngComm*, **16**, 4194 (2014).
[3] S. Chattopadhyay, M.S. Ray, M.G.B. Drew, A. Figuerola, C. Diaz, A. Ghosh. *Polyhedron*, **25**, 2241 (2006).
[4] Q. Gao, Y.-B. Xie, M. Thorstad, J.-H. Sun, Y. Cui, H.-C. Zhou. *CrystEngComm*, **13**, 6787 (2011).
[5] C. Biswas, M.G.B. Drew, E. Ruiz, M. Estrader, C. Diaz, A. Ghosh. *Dalton Trans.*, **39**, 7474 (2010).
[6] M. Zbiri, S. Saha, C. Adhikary, S. Chaudhuri, C. Daul, S. Koner. *Inorg. Chim. Acta*, **359**, 1193 (2006).
[7] S. Shit, P. Talukder, J. Chakraborty, G. Pilet, M.S.E. Fallah, J. Ribas, S. Mitra. *Polyhedron*, **26**, 1357 (2007).
[8] C. Adhikary, D. Mal, R. Sen, A. Bhattacharjee, P. Gütlich, S. Chaudhuri, S. Koner. *Polyhedron*, **26**, 1658 (2007).
[9] Y.-Y. Zhu, C. Cui, N. Li, B.-W. Wang, Z.-M. Wang, S. Gao. *Eur. J. Inorg. Chem.*, 3101, (2013).
[10] S. Mukherjee, B. Gole, Y. Song, P.S. Mukherjee. *Inorg. Chem.*, **50**, 3621 (2011).
[11] S. Banerjee, C. Adhikary, C. Rizzoli, R. Pal. *Inorg. Chim. Acta*, **409**, 202 (2014).
[12] Q.-X. Jia, M.-L. Bonnet, E.-Q. Gao, V. Robert. *Eur. J. Inorg. Chem.*, 3008, (2009).
[13] M. Das, B.N. Ghosh, A. Valkonen, K. Rissanen, S. Chattopadhyay. *Polyhedron*, **60**, 68 (2013).
[14] P.K. Bhaumik, K. Harms, S. Chattopadhyay. *Polyhedron*, **68**, 346 (2014).
[15] P.K. Bhaumik, K. Harms, S. Chattopadhyay. *Inorg. Chim. Acta*, **405**, 400 (2013).
[16] P. Bhowmik, H.P. Nayek, M. Corbella, N. Aliaga-Alcalde, S. Chattopadhyay. *Dalton Trans.*, **40**, 7916 (2011).
[17] X.-Y. Song, W. Li, L.-C. Li, D.-Z. Liao, Z.-H. Jiang. *Inorg. Chem. Commun.*, **10**, 567 (2007).
[18] P. Bhowmik, A. Bhattacharyya, K. Harms, S. Sproules, S. Chattopadhyay. *Polyhedron*, **85**, 221 (2015).
[19] P.S. Mukherjee, S. Dalai, E. Zangrando, F. Lloret, N.R. Chaudhuri. *Chem. Commun.*, 1444, (2001).
[20] S. Chattopadhyay, M.G.B. Drew, C. Diaz, A. Ghosh. *Dalton Trans.*, 2492, (2007).
[21] C.-B. Tang. *Acta Cryst.*, **E63**, m2654 (2007).
[22] CrysAlisPro, Agilent Technologies (Version 1.171.36.21) Yarnton (2012).
[23] R.C. Clark, J.S. Reid. *Acta Crystallogr. Sect. A: Found. Crystallogr.*, **51**, 887 (1995).
[24] L. Palatinus, G. Chapuis. *J. Appl. Crystallogr.*, **40**, 786 (2007).
[25] L.J. Farrugia. *J. Appl. Crystallogr.*, **32**, 837 (1999).
[26] G.M. Sheldrick. *Acta Crystallogr. Sect. A: Found. Crystallogr.*, **64**, 112 (2008).
[27] L.J. Farrugia. *J. Appl. Crystallogr.*, **30**, 565 (1997).
[28] C.F. Macrae, I.J. Bruno, J.A. Chisholm, P.R. Edgington, P. McCabe, E. Pidcock, L. Rodriguez-Monge, R. Taylor, J. van de Streek, P.A. Wood. *J. Appl. Crystallogr.*, **41**, 466 (2008).
[29] M.A. Spackman, D. Jayatilaka. *CrystEngComm*, **11**, 19 (2009).
[30] F.L. Hirshfeld. *Theor. Chim. Acta*, **44**, 129 (1977).
[31] H.F. Clausen, M.S. Chevallier, M.A. Spackman, B.B. Iversen. *New J. Chem.*, **34**, 193 (2010).
[32] A.L. Rohl, M. Moret, W. Kaminsky, K. Claborn, J.J. McKinnon, B. Kahr. *Cryst. Growth Des.*, **8**, 4517 (2008).
[33] A. Parkin, G. Barr, W. Dong, C.J. Gilmore, D. Jayatilaka, J.J. McKinnon, M.A. Spackman, C.C. Wilson. *CrystEngComm*, **9**, 648 (2007).
[34] M.A. Spackman, J.J. McKinnon. *CrystEngComm*, **4**, 378 (2002).
[35] S.K. Wolff, D.J. Grimwood, J.J. McKinnon, D. Jayatilaka, M.A. Spackman, *Crystal Explorer 3.0*, University of Western Australia, Perth (2007). Available online at: http://www.hirshfeldsurface.net/
[36] J.J. McKinnon, M.A. Spackman, A.S. Mitchell. *Acta Crystallogr. Sect. B: Struct. Sci.*, **60**, 627 (2004).
[37] P. Wang, Y.-Y. Wang, Y.-H. Chi, W. Wei, S.-G. Zhang, E. Cottrill, J.-M. Shi. *J. Coord. Chem.*, **66**, 3092 (2013).
[38] Y.-Y. Liu, W.-J. Gong, J.-C. Ma, J.-F. Ma. *J. Coord. Chem.*, **66**, 4032 (2013).
[39] M.-J. Niu, D.-W. Sun, H.-H. Li, Z.-Q. Cao, S.-N. Wang, J.-M. Dou. *J. Coord. Chem.*, **67**, 81 (2014).
[40] Y.-Y. Wang, Q.-H. Liu, W. Wei, H. Du, J.-M. Shi, Y.-Q. Zhang. *J. Coord. Chem.*, **66**, 254 (2013).
[41] Q.-R. Cheng, P. Li, H. Zhou, Z.-Q. Pan, Z.-G. Xu, G.-Y. Liao, J.-Z. Chen. *J. Coord. Chem.*, **67**, 1584 (2014).
[42] S. Jana, B.K. Shaw, P. Bhowmik, K. Harms, M.G.B. Drew, S. Chattopadhyay, S.K. Saha. *Inorg. Chem.*, **53**, 8723 (2014).
[43] M.S. Ray, A. Ghosh, R. Bhattacharya, G. Mukhopadhyay, M.G.B. Drew, J. Ribas. *Dalton Trans.*, 252 (2004).

[44] S. Naiya, S. Biswas, M.G.B. Drew, C.J. Gómez-García, A. Ghosh. *Inorg. Chim. Acta*, **377**, 26 (2011).
[45] P. Mukherjee, O. Sengupta, M.G.B. Drew, A. Ghosh. *Inorg. Chim. Acta*, **362**, 3285 (2009).
[46] S. Koner, S. Saha, T. Mallah, K.-I. Okamoto. *Inorg. Chem.*, **43**, 840 (2004).
[47] R.-H. Hui, P. Zhou, Z.-L. You. *Ind. J. Chem.*, **48A**, 1102 (2009).
[48] Z.-L. You, X.-L. Ma, S.-Y. Niu. *J. Coord. Chem.*, **61**, 3297 (2008).
[49] L.-L. Ni, Z.-L. You, L. Zhang, C. Wang, K. Li. *Transition Met. Chem.*, **35**, 13 (2010).
[50] L.H. Wang. *Russ. J. Coord. Chem.*, **37**, 40 (2011).
[51] P. Mukherjee, M.G.B. Drew, A. Ghosh. *Eur. J. Inorg. Chem.*, 3372 (2008).
[52] B. Sarkar, M.S. Ray, M.G.B. Drew, C.-Z. Lu, A. Ghosh. *J. Coord. Chem.*, **60**, 2165 (2007).
[53] Z.-L. You, H.-L. Zhu. *Z. Anorg. Allg. Chem.*, **630**, 2754 (2004).
[54] A.W. Addison, T.N. Rao, J. Reedijk, J. van Rijn, G.C. Verschoor. *J. Chem. Soc. Dalton Trans.*, 1349 (1984).
[55] J.C.A. Boeyens. *J. Cryst. Mol. Struct.*, **8**, 317 (1978).
[56] M. Das, S. Chatterjee, S. Chattopadhyay. *Inorg. Chem. Commun.*, **14**, 1337 (2011).
[57] M. Das, B.N. Ghosh, K. Rissanen, S. Chattopadhyay. *Polyhedron*, **77**, 103 (2014).
[58] M. Das, S. Chatterjee, K. Harms, T.K. Mondal, S. Chattopadhyay. *Dalton Trans.*, **43**, 2936 (2014).
[59] M. Das, S. Chattopadhyay. *Transition Met. Chem.*, **38**, 191 (2013).
[60] M. Das, K. Harms, S. Chattopadhyay. *Dalton Trans.*, **43**, 5643 (2014).
[61] M. Das, S. Chattopadhyay. *J. Mol. Struct.*, **1051**, 250 (2013).
[62] M.A. Spackman, P.G. Byrom. *Chem. Phys. Lett.*, **267**, 215 (1997).
[63] J. Comarmond, P. Plumere, J. Lehn, Y. Agnus, R. Louis, R. Weiss, O. Kahn, I. Morgenstern-Badarau. *J. Am. Chem. Soc.*, **104**, 6330 (1982).